CREEP DAMAGE DISTRIBUTION IN SILICON NITRIDE BY SLAM

F. Lofaj

Abstract
Scanning laser acoustic microscopy (SLAM) was used to visualize creep damage distribution in the gas-pressure-sintered silicon nitride after creep at 1300°C in 4-point bending. SLAM revealed asymmetrical distribution of creep damage with high concentration of creep cavities beneath the tensile surface and in a narrow zone that spread continuously across the neutral axis toward the compression surface. This is a direct evidence of cavitation asymmetry in vitreous bonded silicon nitride.
Keywords: Scanning laser acoustic microscopy, Silicon nitride, Bending creep, Creep damage distribution, Cavitation asymmetry.

INTRODUCTION

Intensive research and development over 20 years in deformation behavior of silicon nitride ceramics pointed out to at least two principal problems. One of them is high sensitivity to stress [1] experimentally observed in many ceramics and lack of understanding of creep asymmetry [2-5]. The stress exponents in silicon nitride and other vitreous bonded ceramics are usually in the range from 5 to 12, which by far exceeds n predicted by theoretical models for diffusion creep. Strong creep asymmetry also does not agree with conventional models [2-7].

The attempts to explain high stress exponents and creep asymmetry are commonly related to different extent of cavitation [5, 8-15]. Recent model of Luecke and Wiederhorn [15] considers cavitation as the main tensile creep mechanism and predicts exponential dependence on stress. Such dependence explains the existence of a wide range of high stress exponents reported by different authors. However, the comparison of tensile and compressive creep rates revealed that both rates converge and creep asymmetry practically disappears at low stresses [4]. The stress exponent approaches unity, cavitation and non-cavitation creep at these conditions became indistinguishable. The understanding of the physical reason for the disappearance of creep asymmetry is unclear.

Simple theoretical analysis showed that all volume of cavities contributes to tensile strain [5], not only one third of the volume as it was assumed earlier [16]. Indeed, variety of independent experimental methods subsequently revealed that cavities can produce more than 70 % of total tensile strain [5, 14, 17-20]. At the same time, uniaxial compressive strain is only due to non-cavitation mechanisms since cavitation fully contributes to the accompanying radial strain [5]. This strain is considerably smaller than in tension and the density changes measured after compressive tests are also lower [4]. Driving force for cavity formation is reduced when external applied stresses are lower. The contribution of cavitation to tensile strain decreases, ratio between cavitation and non-cavitation mechanisms shifts from >70 % toward smaller values and ultimately, the same non-cavitation mechanisms will produce tensile and compressive strains as well.

František Lofaj, Institute of Materials Research of the Slovak Academy of Sciences, Košice, Slovakia

Bending is experimentally very simple method for simultaneous investigation of both tensile and compressive deformation in one sample. The visualization of the cavity distribution in bending specimen would be useful for approving or disapproving the ideas involved in cavitation creep models. The aim of this paper is to visualize bending creep damage distribution in gas-pressure-sintered silicon nitride at the late stage of deformation using scanning laser acoustic microscopy.

EXPERIMENTAL PROCEDURE

The material studied was prepared from commercial silicon nitride powder LC 12 SX (H.C. Starck) and additives of 9 wt. % of Y_2O_3 and 1 wt. % of Al_2O_3 (H.C. Starck) at IKTS (Fraunhofer - Einrichtung für keramische Technologien und Sinterwerkstoffe, Dresden, Germany). The 5 mm x 6 mm x 60 mm bars were formed by cold pressing at 200 MPa and sintered at 1900 °C and pressure of 50 bars for 90 minutes. The bending specimens with the dimensions 3 mm x 3 mm x 45 mm were cut from the sintered bars and their surfaces were ground by diamond wheels.

Four point bending tests were carried out in argon in bending creep test furnace (HTTF1A, SFL-Instron, Inc., UK) with lever arm and dead weight loading. The outer/inner spans between rollers were 40 mm and 20 mm, respectively. Testing temperature of 1300°C and initial outer fiber stress 65 MPa in flowing argon were chosen based on the results of earlier 4-point-bending creep study [21]. Creep test was interrupted and the specimen was cooled down under load after 0.75 h and then after 8.5 hours of creep exposure. They corresponded to approximately 7.5% and 85% of the lifetime, respectively.

Scanning laser acoustic microscopy

The initial state of the specimen and the state of the creep exposed specimens were investigated after each interrupted creep test were investigated by scanning laser acoustic microscope (Sonoscope 2140, Sonoscan Inc. Bensenville, Chicago, USA) at CNRSM. The scanning laser acoustic microscope (SLAM) used continuous plane ultrasonic waves with the frequency of 100 MHz in transmission mode to detect the changes of the microstructure or the defects in the sample. A scanning laser beam was used as an ultrasonic detector [29]. The distribution of the defects was determined from the relative gray level of pixels after the digitalization of the SLAM image. The darker zones corresponded to higher attenuation of ultrasonic waves on the defects in the microstructure. The difference in gray level of pixels between the zones of tensile and compressive stresses indicated indirectly size and/or relative concentration of defects.

SLAM technique is unable to visualize individual defects in the microstructure due to their overlapping in transmission mode. The defects were identified by transmission electron microscope (TEM) operating at 200 kV (model 2010, JEOL, Japan) on thin foils prepared from the zone beneath the tensile surface.

RESULTS

SLAM observation

The as-received material exhibited relatively homogeneous distribution of ultrasonic attenuation over the whole sample. Only small microstructure changes were found after short time (0.75 hour) creep deformation beneath the surface subjected to tensile strain. Fig. 1 indicates considerable differences in the ultrasonic attenuation after 8.5 hours of creep testing in the same zone whereas the zone subjected to compression stresses revealed homogeneous attenuation except relatively narrow central area. The distribution of

creep damage in different areas of the bending bar was estimated from the histograms. The results of the quantification of the gray level of the pixels with the same intensity from digitized images are schematically shown in Fig. 2. Two principally different areas were obtained: 1- the zone subjected to tensile stresses with high ultrasonic attenuation, which corresponds to high concentration of creep damage, and 2 - the zone with compressive or zero stresses with low attenuation and low concentration of creep damage. Frame 3 indicates the area of the specimen shown in the acoustical micrograph in Fig. 1. Note an irregularity in damage distribution in the center of the sample, which is symmetrically extended from tensile zone into compressive zone.

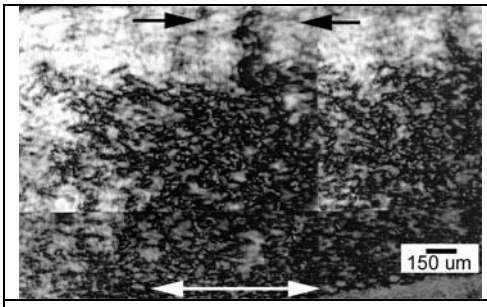

Fig.1. SLAM micrographs of the GPS silicon nitride after the creep at 1300°C under stress of 65 MPa for 8.5 hours. The darker zone below the tensile surface corresponds to higher ultrasonic attenuation due to the presence of creep damage.

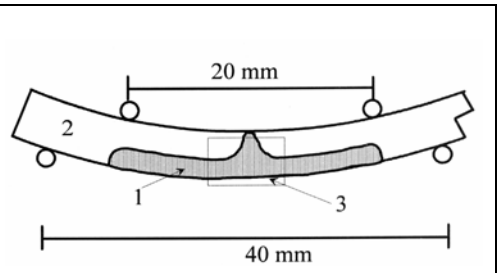

Fig. 2. Schematic distribution of creep damage in the bending bar after creep 1300°C/65 MPa/8.5 hours. Two zones are indicated: 1 - zone with high concentration of creep damage, and 2 - zone with low concentration of creep damage. Frame 3 corresponds to the area shown on Fig. 1.

TEM study

TEM observation revealed very high concentration of creep cavities in the zone of tensile stresses. Cavities were formed inside the glassy phase both at multigrain junctions (Fig. 3 (A)) and two-grain junctions (Fig. 3 (B)). The size of multigrain junction cavities was comparable with the grain size, while the size of oblate cavities on grain facets was considerably smaller.

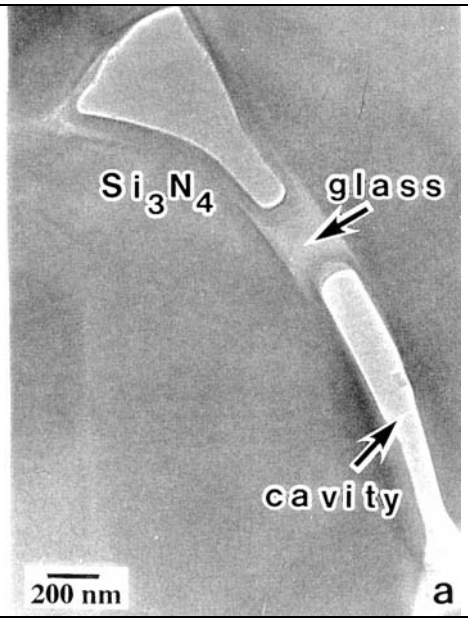

Fig. 3. TEM micrographs of the creep cavities formed in amorphous phase at multigrain junctions (A) and two-grain junctions – (B). The different size of cavities indicates different time of their nucleation and/or different growth rate. The rounded cavity tips in both cases suggest that viscous mechanism of their growth.

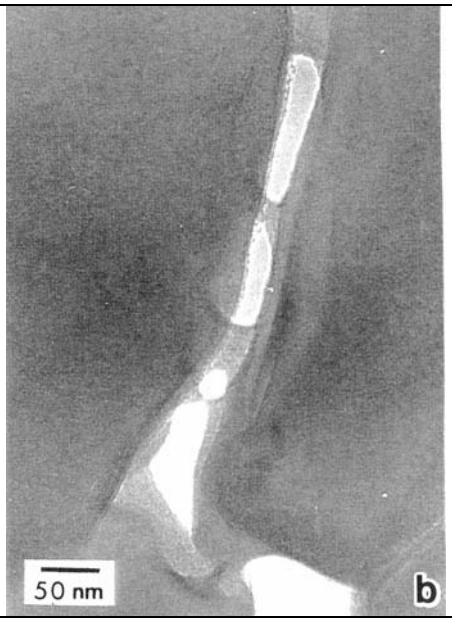

Fig.4. Schematic illustration of bending creep damage development at the late stage of deformation: homogeneous creep damage in the zone of tensile stresses and creep damage zone ahead of the main crack.

DISCUSSION

SLAM and TEM observations of microstructure changes after creep deformation revealed the presence of creep damage and intensive cavitation, respectively. Despite TEM itself is unable to determine the quantitative differences in the concentration of the cavities in different zones and SLAM yields only the integrated image of creep defects, the comparison of both methods suggests that SLAM indirectly visualizes distribution of creep cavities.

Cavitation occurs most easy in the amorphous phase when critical local stress level is reached. Therefore, the attenuation distribution revealed by SLAM should be related to the distribution of critical local tensile stresses for cavity nucleation. However, since the nuclei size is considerably smaller than the detection limit of the acoustic microscopy, the distribution in Fig. 2 relates to the distribution of large cavities.

According to Fig. 2, creep damage developed nonsymmetrically with regard to neutral axis of specimen. The zone of tensile stresses was much more damaged than the zone of compressive stresses. Thus, besides asymmetry in creep rates well known in ceramics, current SLAM observation provides direct quantitative evidence of asymmetry in creep cavitation between tension and compression. The received cavitation asymmetry is in good agreement with the cavitation creep model [15] based on the formation of high

dilatation tensile stresses at some multigrain junctions after local grain boundary sliding (GBS). However, the presence of some cavities in the zone of compression cannot be excluded since GBS results in development of dilatational hydrostatic tensile stresses even at the multigrain pockets in this zone. Evidently, nonsymmetrical creep damage distribution indicates also a difference in the conditions for cavity growth and further evolution throughout the bending bar.

The extension of the creep damage zone through the specimen neutral axis zone into the zone of compressive stresses in the relatively narrow central part of specimen is contrary to the above considerations (see Fig. 2). The width of this zone is considerably smaller than the inner rollers span. Damage theory [23] assumes crack formation only under tensile stresses, which excludes the formation of cavities in the narrow area of compressive stresses and near neutral axis. The reason for this irregularity can be connected with the existence of some large creep crack, which locally increased the stress level and enhanced cavitation, as suggested in Fig. 4. At the early stages of creep deformation, cavities formed homogeneously in the zone beneath tensile surface. Considerably higher cavity growth rate in the region of tensile stresses in comparison with the zone of compressive stresses led to enhanced creep damage development beneath the tensile surface in between inner rollers. At the later stage of deformation, coalescence of cavities results in the formation of main crack. The case becomes similar to the notched or pre-cracked specimen when the crack velocity toward compression surface is controlled by the stress intensity factor [7]. The elastic field at the crack tip changed the level of constraints and promoted fast growth of cavities ahead of crack tip and its slow propagation toward compression surface. This process is restricted to the small region of the "process zone" at the crack tip. While creep damage at the relatively early stage of deformation was the result of continuous growth of cavities in the zone with sufficiently high tensile stresses, after the formation of the main crack, their development was limited mainly to the damage zone at the crack tip.

CONCLUSIONS

SLAM observation of the gas pressure sintered silicon nitride crept in 4-point bending visualized the resulting damage distribution in the bending specimen at different stages of deformation. TEM studies showed that this damage corresponds mainly to the cavities. High concentration of creep cavities was observed beneath the specimen surface, which was subjected to tensile stresses and in narrow zone that spread continuously across the neutral axis toward the surface subjected to compression. The suppression of cavitation was seen in the adjacent zones. The difference in creep damage development in the zones of tensile and compressive stresses was assumed to be related to the distribution of constraints between tension and compression. The model based on the transition from the homogeneous creep cavity development to the damage zone formation ahead of main crack was proposed to explain the presence of creep damage near neutral axis and narrow zone of compressive stresses on the late stage of lifetime. Current SLAM observation is direct the evidence of asymmetry in cavity development during creep in vitreous bonded ceramics.

ACKNOWLEDGMENT

The authors are very grateful to H. Klemm and M.Herrmann (IKTS, Dresden, Germany) for the supply of specimens, to V. Luprano (CNRSM, Brindisi, Italy) for SLAM observation and to M. Reece (QMW, University of London, UK), for the assistance with TEM study. The work was partially supported by VEGA Grant No. 2/7011/20.

References

[1] Wiederhorn, SM.: J. Eur. Ceram. Soc., vol. 22, 2002, in print
[2] Lange, FF.: In Deformation of Ceramic Materials. Ed. R.C.Bradt, et al. , New York : Plenum Press, 1975, p. 361
[3] Ferber, MK., Jenkins, MG., Tennery, VJ.: Ceram. Eng. Sci. Proc., vol. 11, 1990, p. 1028
[4] Soon, KJ., Wiederhorn, SM., Luecke, WE.: J. Am. Ceram. Soc., vol. 83, 2000, no. 8, p. 2017
[5] Lofaj, F., Okada, A., Kawamoto, H.: J. Am. Ceram. Soc., vol. 80, 1997, no. 6, p. 1619
[6] Fett, T., Keller, K., Munz, D.: J. Mat. Sci., vol. 23, 1988, p. 467
[7] Chen, CF., Chuang, TJ.: J. Am. Ceram. Soc., vol. 73, 1990, no. 8, p. 2366
[8] Evans, AG., Rana, A.: Acta Metall., vol. 28, 1980, no. 2, p. 129
[9] Marion, JE., Evans, AG., Drory, MD., Clarke, DR.: Acta Metall., vol. 31, 1983, no. 10, p. 1445
[10] Thouless, MD., Evans, AG.: Acta Metall., vol. 34, 1986, no. 1, p. 23
[11] Chan, KS., Page, RA.: J. Am. Ceram. Soc., vol. 76, 1993, no. 4, p. 803
[12] Chen, CF., Wiederhorn, SM., Chuang, TJ.: J. Am. Ceram. Soc., vol. 74, 1991, no. 7, p. 1658
[13] Chuang, TJ., Wiederhorn, SM.: J. Am. Ceram. Soc., vol. 71, 1988, no. 7, p. 595
[14] Luecke, WE., Wiederhorn, SM., Hockey, BJ., Krause, RE., Long, GG.: J. Am. Ceram. Soc., vol. 78, 1995, no. 8, p. 2085
[15] Luecke, WE., Wiederhorn, SM.: J. Am. Ceram. Soc., vol. 82, 1999, no. 10, p. 2769
[16] Gasdaska, CJ.: J. Am. Ceram. Soc., vol. 77, 1994, no. 8, p. 2408
[17] Wiederhorn, SM.: Z. Metallkd., vol. 90, 1999, no. 12, p. 1053
[18] Okada, A., Lofaj, F.: J. Eur. Ceram. Soc., vol. 20, 2000, no. 10, p. 1521.
[19] Cao, JW., Lofaj, F., Okada, A.: J. Mat. Sci., vol. 36, 2001, p. 1301
[20] Lofaj, F., Smith, DT., Blessing, GV., Luecke, WE., Wiederhorn, SM.: J. Mater. Sci., to be published.
[21] Lofaj, F., Dusza, J., Herrmann, M., Klemm, H.: Forschrittberichte der DKG, vol. 9, 1994, no. 4, p. 29
[22] Kessler, LW.: Proceedings of IEEE, vol. 67, 1978, no. 4, p. 526
[23] Rosenfield, AR., Duckworth, WH., Shetty, DK.: J. Am. Ceram. Soc., vol. 68, 1985, no. 9, p. 483